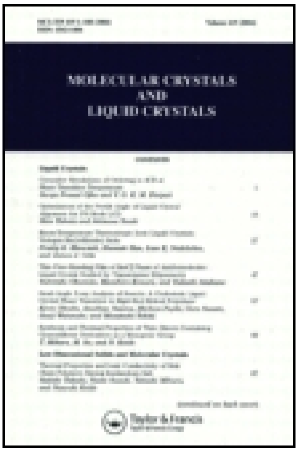

Molecular Crystals and Liquid Crystals
Publication details, including instructions for authors and subscription information:
http://www.tandfonline.com/loi/gmcl20

Liquid Crystal/ITO/Glass System Characterization Obtained by X-Ray Reflectivity Measurements

Stefano Peruzzi [a] , Elza Bontempi [a] , Carlo Versace [b] & Laura Eleonora Depero [a]

[a] INFM, Unità di Brescia, Structural Chemistry Laboratory, Dipartimento di Ingegneria Meccanica, Università di Brescia, Via Branze 38, Brescia, 25123, Italy

[b] INFM, Unità di Cosenza, Dipartimento di Fisica, Università della Calabria, Arcavacata di Rende (Cosenza), 1-87036, Italy

To cite this article: Stefano Peruzzi, Elza Bontempi, Carlo Versace & Laura Eleonora Depero (2002): Liquid Crystal/ITO/Glass System Characterization Obtained by X-Ray Reflectivity Measurements, Molecular Crystals and Liquid Crystals, 372:1, 339-352

To link to this article: http://dx.doi.org/10.1080/713738172

Mol. Cryst. and Liq. Cryst., 2001, Vol. 372, pp. 339-352

Liquid Crystal/ITO/Glass System Characterization Obtained by X-Ray Reflectivity Measurements

STEFANO PERUZZI[a], ELZA BONTEMPI[a], CARLO VERSACE[b]
and LAURA ELEONORA DEPERO[a§]

[a]*INFM, Unità di Brescia, Structural Chemistry Laboratory,*
Dipartimento di Ingegneria Meccanica, Università di Brescia,
Via Branze 38, 25123 Brescia, Italy and
[b]*INFM, Unità di Cosenza, Dipartimento di Fisica,*
Università della Calabria, 1-87036 Arcavacata di Rende (Cosenza), Italy
[§]*ref. author Depero e-mail: depero@bsing.ing.unibs.it*

Abstract The functional properties of liquid crystal (LC) thin films are correlated to their structure and microstructure. Moreover, not only phase and order of LC are important parameters influencing these properties, but also thickness, density, and roughness of the film.

In this paper a study of multilayer systems LC/ITO/glass based on GIXRD (Glancing Incidence X-Ray Diffraction) and XRR (X-Ray Reflectivity) experiments is proposed. It is shown that the nominal thickness of the ITO layers may be wrong. The determination of this parameter and, generally, the structural characterization of the display can be performed by XRR and GIXRD. Moreover, also very thin layer as SiO_x obliquely evaporated for the LC alignment, can be precisely determined.

Keywords XRR (X-Ray Reflectivity); GIXRD (Glancing Incidence X-Ray Diffraction); alignment layer; liquid crystal; ITO

INTRODUCTION

A liquid crystal cell wall usually consists on the glass substrate, the SiO_2 passivation layer (100-2000 nm), the ITO (Indium-Tin Oxide) electrode (150-1000 Å), and the alignment layer. The silicon dioxide layer prevents migration of alkaline ions from the bulk glass to the surface when a soda-lime glass is used. Another SiO_2 layer (150-300 nm) may be deposited above the ITO (and below the alignment layer) to obtain pure capacitive behaviour and to avoid electrical shorts due to conductive impurities inside the cell [1].

For LC devices, an important condition to work is a good surface alignment of liquid crystal molecules. Alignment and tilt angles have a dramatic impact on the electro-optical performance of LCDs.

Homogeneous (parallel) alignment is obtained as long as the surface is microscopically flat and the liquid crystal doesn't contain amphiphilic impurities. Moreover a low surface polarity must be reached by a polymer coating or another coupling agent. The surface is then rubbed to get an unidirectional alignment of the LC molecules. An appropriate molecular pretilt angle is necessary to obtain a domain-free orientation in an electric field.

Film uniformity and substrate influence the functional properties. Moreover, film must be thin to avoid an excessive potential drop and the consequent contrast decreasing in the picture element. Polyimide (PI) rubbed films are the standard to align LCs parallel with some pretilt, because they are easy to use, stable and they can be reproduced. The thickness of this layer is typically 500-800 Å. Another coupling agent is PVA (polyvinyl alcohol).

Langmuir-Blodgett films can be deposited for orienting LC molecules without rubbing [2].

The structural and physical features of all these layers are determining the device performances and then their precise and accurate characterization is mandatory.

In these years, two non-distructive techniques have found large application in structural and microstructural characterization of the films: glancing angle x-ray diffraction (GIXRD) and x-ray reflectivity (XRR). By GIXRD the crystallinity and the orientation of the LC can be determined, while by means of XRR experiments thickness, density and roughness of the film can be calculated. The latter technique is also mandatory for the characterization of the buffer layer, often deposited on the substrate to induce a specific phase or orientation of the LC layer.

Moreover, in principle, the parameters describing the order and the orientation of the LC are related to the refractive index and then can be guessed by XRR data.

X-rays can be specularly reflected from plane surfaces. This is related to the fact that at short wavelength characteristic of X-rays the diffraction index of the material is slightly less than one, making it possible to have total reflection of X-rays at the air/material interface.

Thorough descriptions of XRR can be found in review papers (see, e.g. [4], and Ref. therein) and in a recent book by V. Holy et al. [5]. At X-ray typical frequencies the diffraction index can be expressed as:

$$n=1-\delta-i\beta \qquad (1)$$

where $\delta=\rho_e e^2\lambda^2/2\pi mc^2$, $\beta=\mu\lambda/4\pi$, ρ_e is the electronic density (Z electron per atom), μ the linear absorption coefficient for energies far from the X-ray absorption threshold, and λ the X-ray wavelength.

Since at typical X-ray energies ($E > 5x10^3$ eV) both δ and β have low values (less than about 10^{-5}), the refraction index is very close, but less than, one and the critical angle θ_c falls in the 0.2°-0.5° range. Therefore for incident angles below θ_c a condition of total reflection is established. From a measure of the critical angle the layer density can be estimated, according to the formula:

$$\theta_c=(2\delta)^{1/2}=\lambda\,(r_0\rho_e/\pi)^{1/2} \qquad (2)$$

where $r_0=e^2/mc^2$ is the classical radius of electron.

Above θ_c a dramatic drop of the reflected intensity is observed, along with oscillations (Kiessig fringes [6]) in the signal. The spacing between the maxima θ_{im} of these oscillations can be related to the samples thickness (t) by considering the formula (see, e.g., [5]):

$$2t\sqrt{\sin^2\theta_{im}-\sin^2\theta_c}=m\lambda \qquad (3)$$

where m is an integer, θ_c is the critical angle of total external reflection of the layer and λ is the wavelength of the X-ray source.

In addition to the Kiessig fringes additional peaks may appear in multilayer samples. These peaks are identified as Bragg reflections resulting from the stack of planes, parallel to the substrate surface, which form the multilayer.

Information on the surface or interface roughness is basically contained into the degree of contrast between fringe intensities.

The aim of this paper is to discuss the potentiality of the XRR and GIXRD techniques in the characterization of LC displays.

EXPERIMENTAL

Glass substrates and glass with ITO layer were used. The organic alignment layer films were deposited onto the substrates by spin coating or dip coating. The X-ray reflectivity and GIXRD measurements were performed on a Bruker "D8 Advance" diffractometer equipped with a reflectometry stage and a Goebel mirror that transforms very efficently the divergent primary beam into a parallel beam and monochromatizes the radiation. The angular accuracy is 0.001° and the angular resolution is better than 0.01°. The Cu k_α line of a conventional x-ray source powered at 40 Kv and 40 mA is used for the experiment.

The experimental data were simulated using the program REFSIM 2.0 [3]. The parameters that have been considered in the modelling and fitting with the XRR measurements are for each layer the thickness, the density and the roughness.

RESULTS AND DISCUSSION

Substrates and substrates with ITO

Two samples consisted in a 1.1 mm soda-lime glass substrate with one side covered by an ITO thin film with different resistance. The nominal ITO resistance was 200 Ω/sq for the sample A and 25 Ω/sq for the sample B. Substrates were cleaned in acetone and then rinsed by using deionized water. As a reference, in FIGURE 1 measurements and simulations of the glass substrate are shown. In FIGURE 1(a) the simulation is performed by considering only a SiO_2 amorphous glass substrate. This simulation is not satisfactory and then a thin layer of silicon dioxide above the glass is introduced in the simulation, shown in FIGURE 1(b). The density obtained by the fitting of the upper layer is close to the nominal SiO_2 density (2.6 g/cm^3) and the simulation appears very good. The SiO_2 film has a thickness of only 1.54 nm. The results are reassumed in TABLE 1.

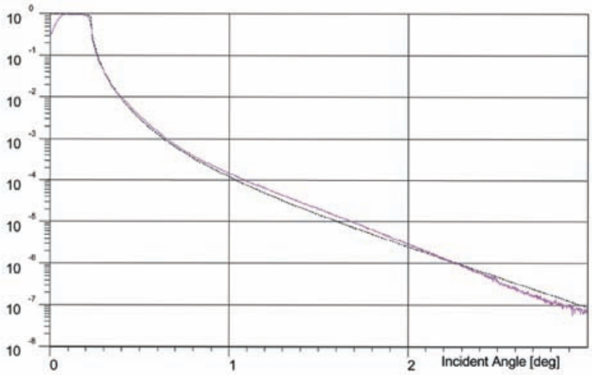

FIGURE 1(a) XRR measurement and simulation (dashed line of a glass substrate without considering overlayers.

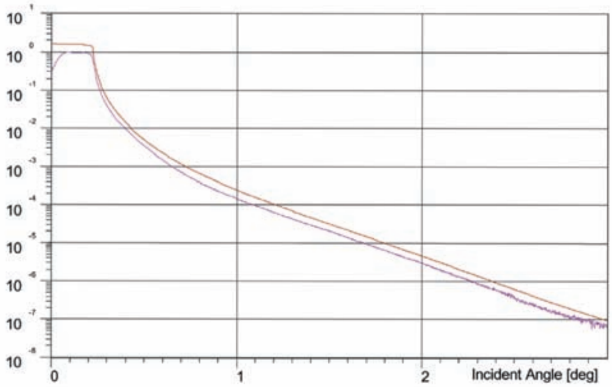

FIGURE 1(b) XRR measurement (bottom curve) of a glass substrate and simulation considering a SiO_2 oxidation film. For the comparison the simulation has been shifted up.

	Thickness [nm]	Roughness [nm]	Density [g/cm^3]
SiO_2	1.54	0.43	2.58
Glass		0.39	2.33

TABLE 1 Structural parameters obtained from XRR simulation for the glass substrate.

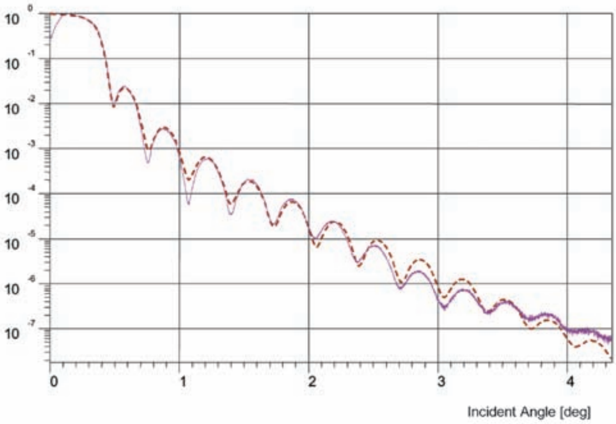

FIGURE 2(a) XRR measurement and simulation (dashed line) of a type A ITO layer.

XRR measurements of the ITO film for two kind of samples are shown in FIGURE 2 (type A in FIGURE 2(a) and type B in FIGURE 2(b)). For both the samples the critical angle is higher then that previously determined for the glass substrate, indicating a higher density value for the ITO in comparison with the glass' one (see TABLE 2).

Type A specimen displays strong and widely spaced Kiessig fringes till 9 degrees in 2è, from which the ITO layer thickness of about 13 nm has been calculated. The density of this layer is about 6.5 g/cm^3 while the roughness is 0.35 nm. It is to be noted that for this sample the nominal thickness is 20 nm.

For sample B a thicker ITO layer (98 nm) and a higher density (7.38 g/cm^3) has been determined. The Kiessig fringes disappear for θ angles higher than 1.5 as a consequence of an higher roughness. From

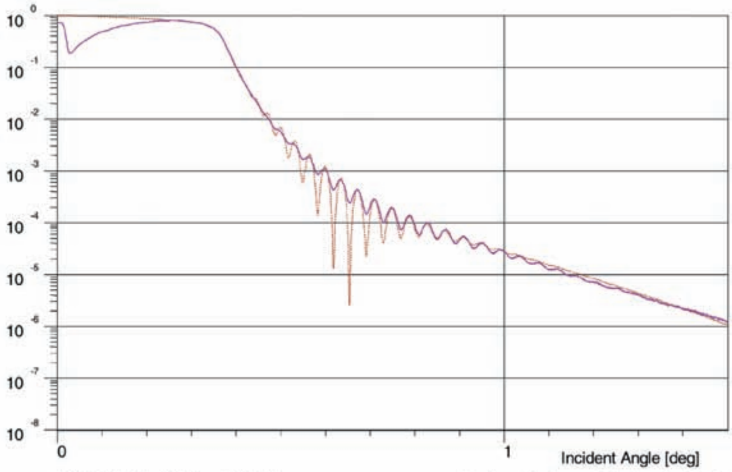

FIGURE 2(b) XRR measurement and simulation (dashed line) of a type B ITO layer.

the fitting the value for this parameter is 2.47 nm. The roughness/thickness ratio is similar for sample A and B (0.027 and 0.025 respectively), probably being a constant of the growth process.

In FIGURE 3 the GIXRD measurements of type A and B ITO specimens are shown. In FIGURE 3(a) GIXRD measurements on a type

Type A	Thickness [nm]	Roughness [nm]	Density [g/cm^3]
ITO	13.13	0.35	6.55
SiO_2	1.63	0.42	2.75
Glass		0.40	2.42

Type B	Thickness [nm]	Roughness [nm]	Density [g/cm^3]
ITO	98.3	2.47	7.38
SiO_2	0.89	0.86	2.60
Glass		0.01	2.40

TABLE 2 Structural parameters obtained from XRR simulation for the type A and type B ITO samples.

B sample were performed with incident angles of 0.5° and 1°. As a reference, the reflections of Indium Oxide (In_2O_3) are reported (JSPDS, card. n. 74-1990).

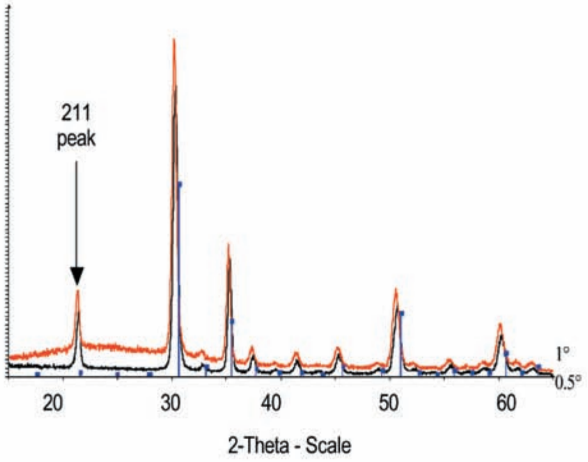

FIGURE 3(a) GIXRD measurements (at 0.5° and 1° incident angle) on a type B sample and peaks for 74-1990 phase of In_2O_3.

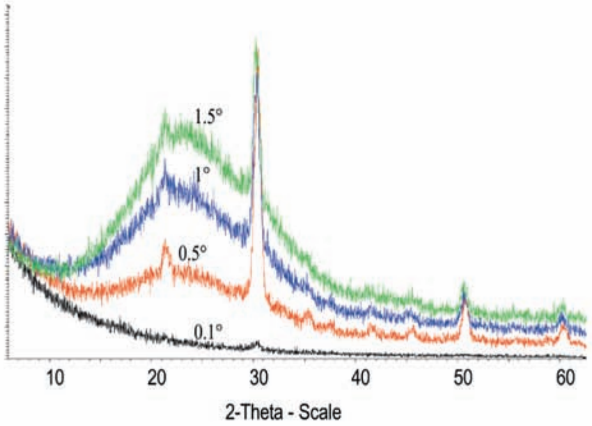

FIGURE 3(b) GIXRD measurements (at 0.1° - 0.5° - 1° - 1.5° incident angle) on a type A sample.

As the incident angle decreases, the halo at 24°, ascribed to the SiO_2 substrate, decreases. In fact, for small incidence angles the GIXRD is more sensitive to the film phases. Moreover, the 2θ position of the ITO reflections decreases with increasing incidence angle, showing different spacing for this phase throughout the sample depth. This fact can be justified by different percentage of Sn in the phase and/or stress in the layer. The high intensity of the 211 peak at 21.5° (2θ), also shown in FIGURE 3(a), cannot be attributed to preferred orientation because does not depend on the incidence angle. Tentatively this effect is attributed to the substitution of Sn in the In_2O_3 phase. In FIGURE 3(b) GIXRD measurements on a type A sample were performed with incident angles of 0.1° - 0.5° - 1° - 1.5°. Since sample A ITO layer is thinner, peaks are less intense than in sample B and the broad halo peaked at 24° of the SiO_2 substrate disappears only for incident angle of 0.1°, when the diffraction experiment is performed on the evanescent wave.

Alignment layers

The common methods used for liquid crystal alignment are obliquely evaporated silicon monoxide, SiO [7], and rubbed polymers [8], as for example the polyimide. In this section, XRR and GIXRD measures of these two types of alignment layers are shown. In particular, in FIGURE 4(a) the XRR measurement and simulation curves of a type B specimen on which a thin SiO_x film was evaporated at 60° (at this angle the film gives a planar alignment) are shown. From the fitting, the SiO_x layer (TABLE 3) has a thickness of 20 nm and a density of 2.1 g/cm^3. The depression at 0.25° after the first plateau (shown in FIGURE 4(a)) is

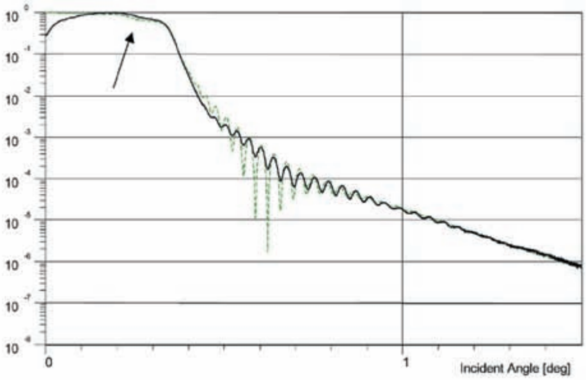

FIGURE 4(a) XRR measurement and simulation curve of a type B ITO specimen with a thin SiO_x film evaporated at 60°.

	Thickness [nm]	Roughness [nm]	Density [g/cm^3]
SiO_x	20.00	4.80	2.06
ITO	103.47	2.48	6.75
SiO_2	1.63	0.74	2.82
Glass		0.01	2.40

TABLE 3 Structural parameters obtained from XRR simulation for type B specimen on which a thin SiO_x film was evaporated at 60°.

due to the change in the density from the SiO_x to the underlying ITO layer. The simulated SiO_x film roughness results very high (5 nm), probably because of the columnar like structure of evaporated SiO_X films [9].

The GIXRD measurements for this sample at different incidence angles (0.2° - 0.3° - 0.4° - 0.5°) are reported in FIGURE 4(b) in the sqrt scale in order to emphasize ITO reflections at small incidence angles.

In the measures at 0.2° and 0.3° incidence angles, the peak at 35.5° has a higher intensity relative to the same peak at higher incidence angles (0.4° and 0.5°), as shown.

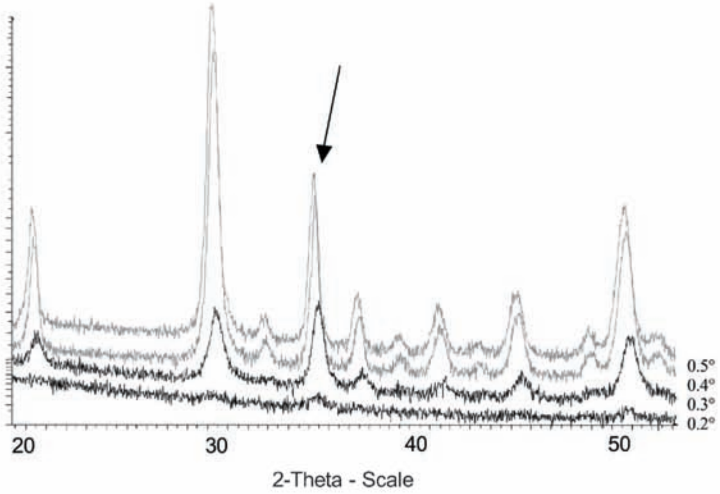

FIGURE 4(b) SiO_x 60° evaporated sample GIXRD measurements at 0.2° - 0.3° - 0.4° - 0.5° in sqrt scale.

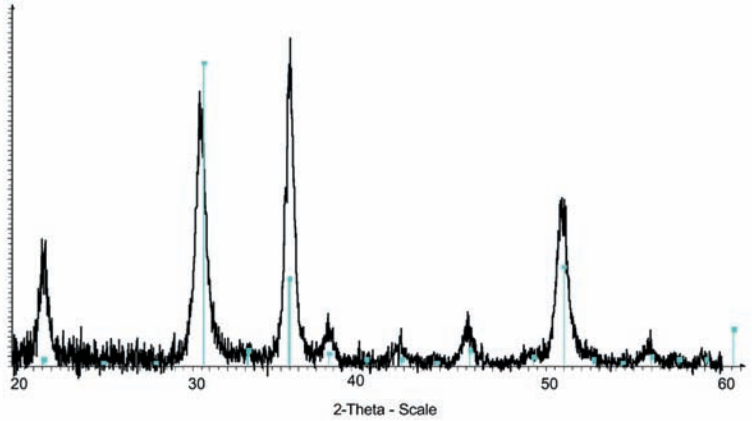

FIGURE 4(c) 0.3° GIXRD measurement and database peaks for 74-1990 In_2O_3 phase.

In FIGURE 4(c) the 0.3° GIXRD measurement and the database peaks for 74-1990 In_2O_3 phase are compared.

Subtracting from the 0.3° measure the ITO (type B) GIXRD measurement at the same incidence angle, the curve in FIGURE 4(d) was obtained. All these reflections belong to the cristobalite phase and thus can be ascribed to a SiO_x upper layer. The intensities do not coincide because of the different stoichiometry of the SiO_x phase and/or preferred orientation of this layer.

In order to characterize the alignment of the liquid crystal by rubbed polymers, X-ray reflectivity measurements were performed on ITO/glass specimens covered with a thin film of a surfactant for homogeneus alignment (ACM72). The film was deposited by dip-coating from a 0.1% solution in deionized water and then baked for 10 minutes at 120°C. FIGURE 5 shows XRR measurements of two samples prepared at the same time, one of which was rubbed with a velvet cloth. In the rubbed sample the alignment layer film is obviously thinner, but the thickness of the sample is very homogenous. This results is different from that for polyimide films whose thickness, measured by reflection ellipsometry, results to be independent of the rubbing [10].

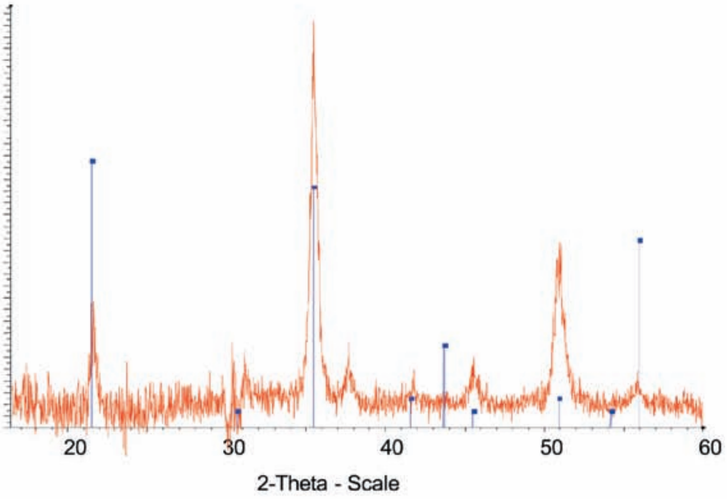

FIGURE 4(d) Subtraction of a sample B 0.3° GIXRD spectrum from the SiO_x sample GIXRD spectrum at the same incidence angle and cristobalite's peaks (dotted lines).

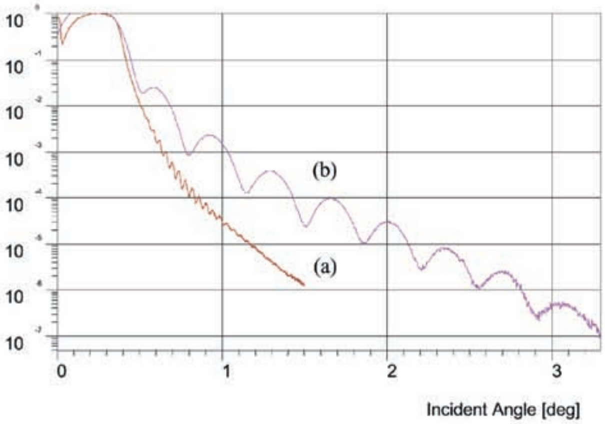

FIGURE 5 XRR measurements of rubbed (b) and unrubbed (a) ACM72 films on ITO/glass substrate.

Liquid crystal films

FIGURE 6 shows the XRR spectra of two MBBA films spin-coated on different substrates. The XRR spectrum of a sample B ITO/glass substrate is reported for comparison (a). The curve (b) is the XRR spectrum of a MBBA film spin-coated on the same substrate. In this case the critical angle is smaller then that of sample B because MBBA density is much lower than the ITO's one, but the Kiessig fringes are due to the ITO underlayer. Indeed, in the pattern of a MBBA film spin-coated on a bare glass substrate (c) the critical angle is the same of that present in curve (b), but no Kiessig fringes are detected.

The possible explanation is that the thickness of the liquid crystal layer is too high to be detected and the absorption coefficient is sufficiently low to see the underlying ITO layer.

CONCLUSION

In this paper a study of multilayer systems LC/ITO/glass based on GIXRD and XRR experiments is proposed.

In conclusion, we showed that these techniques are extremely sensitive tool for the non destructive thin films analysis. The extracted information are also complementary. The structural parameters of all the films are extremely important for a complete characterization of the device.

In particular these techniques are fundamental to understand the structural properties of the ITO layers and it was showed that the electrical measurements are not sufficient for an accurate and precise determination of the film thicknesses. Moreover, even after the liquid crystal deposition the thickness of the ITO film can be easily tested.

It was shown that even the very thin layer of SiO_x, obliquely evaporated for the liquid crystal alignment, can be detected and characterised, both by XRR, determining thickness, density and roughness, and GIXRD, showing that, indeed, these upper layer is formed by a crystalline phase, related to the crystobalite.

Moreover, the thickness of ACM72 films is smaller after the rubbing even if very homogeneous films are obtained by this procedure.

References

[1] S. Morozumi, "Materials and assembling process of LCDs", Liquid crystals applications and uses, Vol. 1, World Scientific, Singapore, (1990)

[2] Ikeno et al., Jpn. J. Appl. Phys., **27**, (1988)

[3] REFSIM 2.0, AGFG, copyright Bruker AXS GmbH 1995-1999

[4] M. Tolan, W. Z. Press, Kristall, **213**:319 (1998)

[5] V. Holy, U. Pietsch, T. Baumbach, High resolution X-ray scattering for thin films and multilayers, Springer, Berlin, (1999)

[6] H. Kiessig, Ann. der Physik (Liepzig), **10**: 769, (1931)

[7] S. Kaho et al., Mol. Cryst. Liq. Cryst., **199**:87, (1991)

[8] B. O. Myrvold, Liq. Crys., **4**:637, (1989)

[9] Goodman et al., IEEE Trans. on Electron Devices, **ED-24** :795, (1977)

[10] I. Hirosawa, Jpn. J. Appl. Phys., **36**, (1997)